Sensors & Diagnostics

PAPER

Check for updates

Single-step colorimetric detection of acid phosphatase in human urine using an oxidase-mimic platinum nanozyme†

Sanjana Naveen Prasad, [iD] Sanje Mahasivam, Sabeen Hashmi,
Vipul Bansal [iD]* and Rajesh Ramanathan [iD]*

Acid phosphatase (ACP) is an important diagnostic biomarker for several diseases, especially those of the prostate and kidney. Nanozyme-based approaches have shown promise in the detection of ACP in human serum. However, the serum ACP levels cannot differentiate between the prostatic and renal ACP levels, and thus do not provide a true reflection of the disease state. To address this challenge, we demonstrate the potential of an oxidase-mimicking Pt nanozyme for the detection of ACP in human urine. The sensing strategy is based on the antioxidant capability of ascorbic acid that is produced *in situ* by the enzymatic activity of ACP and inhibits the nanozyme-mediated oxidation of the chromogenic substrate. Notably, the high activity of the Pt nanozyme across a wide pH range allowed the typical two-step ACP assay to be performed in a single step. This could reduce the assay time by half to 20 min. The deployment potential of this Pt nanozyme ACP sensor in complex biological fluids is demonstrated by estimating ACP in human urine samples in the 2–80 mU mL^{-1} range, a concentration that is conducive to differentiating between a healthy and diseased scenario. The simplicity of a rapid, one-step, colour-based ACP detection method facilitated by Pt nanozyme offers potential applicability in clinical diagnostics of kidney and prostatic diseases.

1. Introduction

Acid phosphatase (ACP) is a biologically active phosphomonoesterase enzyme found in mammalian body fluids and tissues. This enzyme regulates a variety of intracellular physiological reactions including the hydrolysis of orthophosphate monoesters and transphosphorylation reactions.[1] The change in the physiological concentration of ACP is regarded as a potential biomarker for the prognosis of several diseases, such as prostate cancer, hyperparathyroidism, Gaucher's disease, and bone-related disorders including Paget's disease.[2,3] Although serum is the most commonly used biological fluid for the detection of ACP,[4] urine could act not only as a non-invasive alternative for ACP detection but also as a more powerful alternative with the ability to differentiate between prostatic and renal ACP. Urine is a rich source of ACP not only due to prostatic secretions in males but also from kidney excretions in

general, more specifically by the glomerulus.[4,5] However, the amount the urinary ACP that is excreted is dependent on the age, sex, and health condition of an individual. Young healthy men were found to excrete up to 4–6 times more urinary ACP than elderly men or women of all ages. Men and women suffering from carcinoma of the prostate and breast, respectively, were observed to excrete lesser urinary ACP despite elevated serum ACP levels.[4,6] The deterioration of renal function was also reported to be accompanied by a decrease in excretion of urinary ACP.[4] Conversely, active proliferative glomerulonephritis was seen to cause elevated urinary ACP excretion, and a variation in urinary ACP levels for various renal diseases was reported.[5] However, the lack of substantial knowledge on relative ACP activity in renal tissues, serum, and urine during renal diseases was also noted.[5] Hence it is imperative to develop sensors and diagnostic technologies for urinary ACP detection not only to monitor renal health but also to understand the relationship between serum ACP and urinary ACP, as well as the relationship between renal and prostatic ACP in male subjects.

To date, several strategies have been employed for ACP detection, such as high-performance liquid chromatography (HPLC), radioimmunoassays, enzyme immunoassays, and counter immunoelectrophoresis methods.[7,8] Many of these require sophisticated instrumental setup or extensive sample

*Sir Ian Potter NanoBioSensing Facility, NanoBiotechnology Research Laboratory (NBRL), School of Science, RMIT University, Melbourne VIC 3000, Australia.
E-mail: vipul.bansal@rmit.edu.au, rajesh.ramanathan@rmit.edu.au;
Tel: +61 3 9925 2121, +61 3 9925 2887*

preparation. More recently, electrochemical, fluorescence, and colorimetric sensors have also been proposed to detect ACP in different biological fluids, including blood, serum, semen, and urine.[3,9-11] These sensors require relatively inexpensive instrumental set-up and are simple to use in terms of sample preparation, sensor operation, and sensor read-out.[12,13] Of these, the use of colorimetric signals for detection is desirable as it allows the incorporation of digital tools including a smartphone photo for image analysis and automation.[14-16]

Conventional colorimetric sensors such as ELISA (enzyme-linked immunosorbent assay) typically rely on an enzyme such as horseradish peroxidase (HRP) for the generation of a quantifiable colorimetric signal.[17] Recent research has seen the use of nanomaterials that mimic the catalytic activity of natural enzymes, commonly called nanozymes, to generate a colorimetric output in sensing applications.[18-34] The use of nanomaterials instead of a natural enzyme such as HRP to catalyse enzymatic reactions have advantages, such as the ability to operate in a wider range of conditions, ease of modifying the surface chemistry of nanoparticles to control its catalytic properties, and facile conjugation of recognition moieties to improve sensor selectivity.[19,35-38] So far, nanozymes with the ability to mimic the catalytic activity of oxidoreductases, hydrolases, lyases, and isomerases have been reported.[18,19,39,40] As of today, nanozymes, therefore, represent four of the six classes of natural enzymes.[32] Among different enzyme mimics, much of the work has focused on oxidoreductases, primarily on peroxidases and oxidases.[19,32,33] A key difference between peroxidase and oxidase nanozymes is that the former requires hydrogen peroxide (H_2O_2) as a co-substrate to catalyse the oxidation of organic substrates.[41] In contrast, oxidase-mimic nanozymes can use ambient O_2 as an electron acceptor.[42] Thus, while

the use of both peroxidase and oxidase nanozymes for sensor development is common, the latter has some obvious advantages due to their operation in the absence of H_2O_2. Firstly, minimising the number of reagents during an assay can simplify the workflow of the assays. Secondly, the high reactivity of H_2O_2 with a range of inorganic nanozymes can influence their integrity during assays. Last, but not least, H_2O_2 can also interfere with the sensing of several biomolecules.[43] Therefore, the use of peroxidase nanozymes may pose challenges during sensor operation, and oxidase nanozymes may offer a preferred platform for developing ACP sensors.

The previous nanozyme sensors for the detection of ACP have conceptually relied upon ascorbic acid generated during ACP-mediated hydrolysis of 2-phospho-L-ascorbic acid (AAP), in acidic medium to block the production of colour during ACP detection.[44] The antioxidant capability of ascorbic acid inhibits the ability of oxidase nanozymes to catalyse the oxidation of colorimetric oxidase substrates into a coloured product during the assay. In nearly all the nanozyme sensors reported for ACP detection, the assay involves two independent steps (Table 1). In the first step, the sample containing ACP is incubated with AAP in mildly acidic conditions at 37 °C to generate ascorbic acid. The oxidase-mimic nanozyme and its colorimetric substrate are then introduced, and the assay conditions are changed for optimal nanozyme activity. This two-step process creates a workflow challenge for the practical deployment of nanozyme-based ACP sensors. We envisage that by employing a nanozyme that can operate at mildly acidic conditions in which the first step operates, we may be able to eliminate the need for a two-step reaction, thereby decreasing the operational complexity and time required for the assay. Another key distinction of the current work from most of the previous studies is the ability

Table 1 Comparison of different nanozyme systems that have been used for ACP detection

Nanozyme		Approach	Detection range [mU mL^{-1}]	Assay time	Sample matrix
PdPt nanowires[44]		Two steps	0.17–2.67	50 min	Bovine serum
Co-single atom[47]		Two steps	0.3–2.5	40 min	Bovine serum
MnO_2 nanosheets[13]		Three steps	0.075–0.45	85 min	Human serum
Chitosan–Pt NPs[9]		Two steps	0.25–2.5	35 min	Human serum
MoO_3 NPs[48]		Two steps	0.09–7.3	60 min	Human serum
CuS nanoclusters[49]		Two steps	0.05–25	19 min	Human serum
AuPd nanoclusters[50]		Two steps	1–14	40 min	Human serum
NH_2-MIL-101 MOF[11]		Two steps	0.01–30	80 min	Human serum
C_3N_4 nanosheets[51]		Two steps	0.05–40	45 min	Human serum
AuNPs[12]		Two steps	0.01–50	40 min	Human serum
Co_3O_4 nanoflowers[52]		Two steps	0.1–25	45 min	Human serum
Fe–N/C single atom[53]		Two steps	0.1–10	40 min	Human serum
Pd–Pt icosahedra[54]		Single step	0.43–10	15 min	Human serum
Pd nanoplates[55]		Single step	0.01–6	35 min	Human serum
Carboxy chitosan–PtNPs[56]		Single step	0.25–18	30 min	Human semen
Carbon dots[57]		Two steps	0.1–5.5	40 min	Human urine
PtNP (current work)	Blue product	Two steps	0.5–12	45 min	Buffer
	Blue product	Single step	0.5–15	15 min	Buffer
	Yellow product	Two steps	0.5–20	50 min	Buffer
	Yellow product	Single step	0.5–20	20 min	Buffer
	Yellow product	Single step	0.5–20	20 min	Human urine (diluted)
	Yellow product	Single step	2–80	20 min	Human urine

of the proposed Pt nanozyme to quantitatively determine ACP concentrations in human urine in a broad dynamic range. The use of urine as the sample matrix not only eliminates the need for invasive sample collection required for serum, more importantly it opens prospects to differentiate between renal and prostatic ACP levels that cannot be determined based on serum and blood analysis. A broad dynamic range of sensor operation is important as it offers improved prospects in differentiating between disease and non-diseased conditions without requiring significant sample dilution. This has become possible by employing citrate-capped Pt nanozyme, as the use of citrate during the synthesis of nanozyme provides monodisperse particles with high stability due to the negative surface charge in most acidic pH ranges.[45,46] Here, we utilised the inherent oxidase-mimic catalytic activity of citrate-capped platinum nanoparticles (PtNPs) which can catalyze the oxidation of TMB to produce a blue charge-transfer complex in the presence of dissolved oxygen (without H_2O_2). The generation of color was inhibited in the presence of ACP due to the antioxidant ability of ascorbic acid in situ produced during the reaction. The assay could be successfully performed in mildly acidic conditions that offered optimal ACP activity and Pt nanozyme activity. The proposed nanozyme sensor could detect ACP in human urine with high confidence and limited matrix effect, as reflected by a recovery of 96–104%.

2. Materials and methods

The experimental methodology and details of materials used in this study are provided in the ESI.† In brief, PtNPs were synthesised by a multistep seed-mediated growth procedure as described by Bigall et al.,[58] and the PtNPs were then characterised using spectroscopy and microscopy tools. The oxidase-mimic catalytic activity of PtNPs was assessed using TMB as the chromogenic substrate followed by assay optimisation by varying the reaction conditions. The steady-state kinetic parameters of the Pt nanozyme were determined by maintaining a fixed concentration of PtNPs while varying the concentration of TMB. The ROS generated by the Pt nanozyme were assessed using different fluorogenic and colorimetric probes. The oxidase-mimic catalytic activity of PtNPs was then used to develop a colorimetric sensor for the detection of ACP where ACP quantification was carried out by three approaches, further elaborated in the ESI.† The mechanism by which ACP modulates the oxidase-mimic nanozyme activity of PtNPs was determined by assessing the effect of ascorbic acid on the catalytic activity of PtNPs. Further, sensor specificity was determined by assessing the ability of the sensor to detect ACP in the presence of potential interfering biomolecules. This was followed by assessing the robustness of the Pt nanozyme sensor to detect ACP in human urine by spiking the sample with predetermined concentrations of ACP.

All experiments involving human samples were performed in accordance with the Guidelines of the RMIT University's Science, Engineering and Health College Human Ethics Advisory Network (CHEAN) as it meets the requirements of the National Statement on Ethical Conduct in Human Research (National Health and Medical Research Council Australia, 2007). Informed consents were obtained from human participants of this study, and samples were collected as per the approved guidelines by CHEAN (project number 25839).

3. Results and discussion

3.1 Characterisation of PtNPs

The size and morphological characteristics of PtNPs were determined by transmission electron microscopy (TEM). TEM analysis confirmed the quasi-spherical morphology of these particles with a diameter between 25–31 nm (Fig. 1a). The crystalline nature of PtNPs was assessed using X-ray diffraction (XRD) (Fig. 1b) which revealed well-defined Bragg reflections corresponding to the (111), (200), (220), and (311) lattice planes of the face-centered cubic (fcc) lattice structure of crystalline Pt.[58] A zeta potential value of −28.2 mV suggests that the particles were capped with citrate molecules during synthesis, resulting in a negatively charged surface. Dynamic light scattering (DLS) measurements revealed a hydrodynamic diameter of ca. 50 nm which is further supportive of the citrate capping of these nanoparticles.

3.2 Oxidase-mimic catalytic activity of Pt nanozymes

The oxidase-mimicking catalytic activity of PtNPs was determined by assessing their capability to oxidise the chromogenic substrate, TMB. The PtNPs could oxidise TMB to a blue charge transfer product (λ_{max} = 652 nm) in the absence of H_2O_2, confirming that the PtNPs mimic the catalytic activity of oxidases (Fig. S1a†). Control experiments in the absence of PtNPs did not show the formation of the blue product. To understand if the oxidation of TMB was indeed due to the intrinsic nanozyme activity of PtNPs or the potentially leached Pt ions, the catalytic activity of potentially leached metal ions in the reaction was assessed. For this, PtNPs were first incubated in a buffer solution (pH 5) and the NPs were extracted via high-speed centrifugation. The
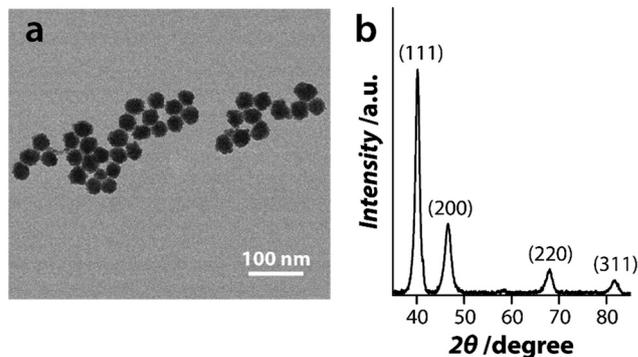

Fig. 1 Characterisation of PtNPs where (a) shows a representative TEM image of the nanoparticles and (b) shows their XRD pattern.

potentially leached ions in the buffer were then used as a catalyst. No colorimetric response was observed suggesting that PtNPs were essential for the catalytic reaction to proceed (Fig. S1a†).

The reaction conditions were optimized by varying the chromogenic substrate, the concentration of the catalyst, the pH, and the temperature at which the reaction occurs. First, PtNPs were exposed to other common chromogenic substrates such as *o*-phenylenediamine dihydrochloride (OPD) and 2,2′-azino-bis(3-ethylbenzothiazoline-6-sulphonic acid) (ABTS) in addition to TMB. The PtNPs could oxidise all three chromogenic substrates to their corresponding products (TMB$_{ox}$ at λ_{max} = 652 nm, OPD$_{ox}$ at λ_{max} = 417 nm, and ABTS$_{ox}$ at λ_{max} = 420 nm) (Fig. S1b†). However, the concentrations of the products were lower in the case of ABTS and OPD compared to that of TMB. Of the three substrates, ABTS was the least preferred substrate showing only 6 μM concentration of the oxidised product. In contrast, the concentration of oxidised TMB and OPD was >15 μM. This suggests that the negatively charged PtNPs favor reacting with positively charged chromogenic substrates such as TMB and OPD.

The nanozyme activity of PtNPs was further optimized by altering the reaction conditions (Fig. S2†). The catalytic activity improved as a function of increasing nanozyme concentration (measured as a function of equivalent Pt ion concentration) (Fig. S2a†). Prominent catalytic activity was observed at a mildly acidic pH of 4 to 5, with the highest activity at pH 4, beyond which the catalytic activity reduced significantly (Fig. S2b†). These observations are similar to those of oxidase-mimic nanozymes and natural enzymes that utilize similar substrates for an assay that are most active under acidic conditions.[19] An interesting result was obtained when we further optimized the reaction temperature. Typically, nanozymes show a temperature-dependent catalytic activity where the activity increases with an increasing temperature (also common for inorganic catalysts).[24] However, the catalytic activity of natural enzymes typically reduces when the temperature of the reaction is outside the optimal range.[38,59] In our case, the reaction temperature had minimal effect on the catalytic activity of PtNP nanozymes. Increasing the temperature above 37 °C reduced the ability of PtNPs to catalyse the oxidation of TMB slightly (Fig. S2c†). Based on these optimizations, we determined that for the optimal oxidase-mimic activity, TMB should be used as a substrate at 37 °C, pH of 4–5 and at the Pt ion concentration of ~12 μM.
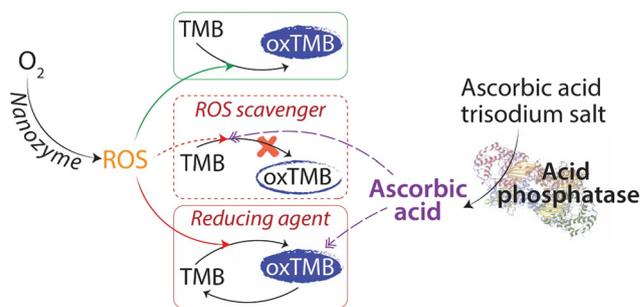
3.3 Steady-state kinetic parameters of PtNPs

The steady-state kinetic parameters of PtNPs were calculated to determine the optimum TMB concentration for the ACP assay. The Michaelis constant (K_m) which is indicative of the affinity of the nanozyme to its substrate, and the maximum initial velocity (V_{max}) that corresponds to the rate at which the nanozyme catalyses the substrate, are two key parameters that define the catalytic efficiency. These steady-state kinetic parameters of Pt nanozymes were determined by varying the TMB concentration. A double reciprocal plot of the substrate concentration [1/S] *vs.* initial velocity [1/V$_0$] (Lineweaver–Burk plot) showed a linear relationship (Fig. S3†). Using the linear equation, the apparent K_m for TMB was calculated to be 180 μM and the V_{max} was calculated to be 3.6×10^{-8} Ms^{-1}. This suggests that the TMB concentration of ~0.2 mM could be ideal for the development of the ACP detection assay.

3.4 Mechanism of oxidase-mimicking catalytic activity of PtNPs

Natural oxidases catalyse redox reactions in the presence of O$_2$ as an electron acceptor by generating reactive oxygen species (ROS) such as H$_2$O$_2$ and superoxide radical (O$_2^{\bullet-}$).[42] H$_2$O$_2$ can also result in the *in situ* generation of hydroxyl radical ($^{\bullet}$OH) during the reaction. Oxidase-mimicking nanozymes follow a similar mechanism to generate ROS; however, the ROS produced is typically either O$_2^{\bullet-}$ or singlet oxygen (^{1}O$_2$).[9,44] Any of these ROS can oxidize the colorimetric substrate, TMB. To understand which ROS is produced during the oxidase-mimic reaction by Pt nanozyme, probes that specifically bind to either $^{\bullet}$OH, O$_2^{\bullet-}$ or ^{1}O$_2$ were used (Fig. S4†). Terephthalic acid (TA) is a fluorogenic probe that binds to $^{\bullet}$OH radicals and gets oxidized to produce a fluorescent 2-hydroxy terephthalic acid, which would result in a fluorogenic signal at 420 nm.[15] Another fluorogenic probe, hydroethidine (HE), is specific for O$_2^{\bullet-}$, and gets oxidized to a fluorescent 2-hydroxyethidium ($\lambda_{emission}$ = 640 nm) if O$_2^{\bullet-}$ is produced during the reaction.[60] In the case of PtNPs, we observed no change in the fluorescence response compared to the control reactions for both $^{\bullet}$OH and O$_2^{\bullet-}$ radical assays (Fig. S4a and b†). This suggests that H$_2$O$_2$ and O$_2^{\bullet-}$ are not involved in the PtNPs-mediated oxidation of TMB. We then employed a colorimetric probe, 9,10-anthracenediyl-bis(methylene)dimalonic acid (ABDA) to assess the generation of ^{1}O$_2$ species.[61] In this case, a colorimetric signal of ABDA with absorbance peaks at λ_{360nm}, λ_{380nm}, and λ_{400nm} is reduced by ^{1}O$_2$ species. The decrease in the absorbance intensity compared to pure ABDA in the presence of PtNPs suggests that ^{1}O$_2$ produced during the

Scheme 1 A schematic representation of the sensing strategy used for ACP detection using PtNPs.

nanozyme catalysed reaction is responsible for the oxidation of chromogenic substrates (Fig. S4c†).

3.5 Colorimetric detection of ACP in buffer

The intrinsic oxidase-mimic catalytic activity of PtNPs was used to develop a colorimetric assay for the detection of ACP. Scheme 1 outlines the sensor mechanism. In the absence of ACP, the Pt nanozyme will oxidize TMB to form the blue charge transfer complex (Scheme 1, green box). However, in the presence of ACP, the enzyme would promote the oxidation of its substrate AAP to inorganic phosphate and ascorbic acid. Ascorbic acid would either inhibit the oxidation of TMB to a blue product due to its ROS scavenging ability (Scheme 1, red dotted box)[48,50,55] or reduce the blue charge transfer complex back to the parent TMB[12,55] (Scheme 1, red box). In both instances, the intensity of the blue color would be reduced, which can be employed for the detection of ACP. Control experiments were conducted to determine the colorimetric response in the absence of AAP or ACP. In both instances, the oxidation of TMB by PtNPs continued unhindered; while in the absence of TMB or PtNPs, no color was generated in the system (Fig. S5†).

As indicated earlier, when nanozymes are used for ACP quantification, a two-step approach is typically required (Table 1) as the reaction conditions for ACP enzyme activity and nanozyme catalytic activity are different. The ACP activity requires an optimum pH of 4.8, while nanozymes operate at more acidic conditions of pH 3–4.[24] Therefore, in the first step, the ACP enzyme and its substrate are incubated in a buffer to maintain a pH of 4.8. This is followed by the addition of the nanozyme and its chromogenic substrate at pH 3–4. We first used this two-step approach for the detection of ACP using Pt nanozyme. Briefly, the ACP enzyme

and its substrate, AAP were first incubated at 37 °C for 30 min in pH 4.8 buffer. Post-incubation, the Pt nanozyme and TMB were added, and the reaction was incubated for a further 15 min in a pH 4 buffer. The intensity of the oxidised product of TMB was measured at 652 nm after incubation. As shown in (Fig. 2 – Blue □), the intensity of the blue product decreased with an increase in the ACP enzyme concentration. This decrease in response showed a linear correlation from 0.5 to 12 mU mL^{-1} ACP concentration, beyond which the sensor response saturated (Fig. S6†). This result is comparable to previous reports using a two-step approach, where a total reaction time of 45 min was typically required (Table 1). To see if we can further reduce the assay time, we considered the possibility of eliminating one of the two steps during sensor operation. We envisaged that by performing the assay using a single buffer that would support the enzymatic activity of acid phosphatase as well as the enzyme-mimic activity of the nanozyme, we could potentially eliminate one of the steps. The optimal catalytic activity of acid phosphatase is reported to be pH 4.8, while the Pt nanozyme showed the highest catalytic activity at pH 4 and a reasonable activity at pH 5. Therefore, using Pt nanozyme, an optimum sensor performance can be potentially achieved between pH 4–5. This simple strategy can not only simplify the assay by eliminating the need for two steps, but it is also expected to reduce the assay time. Thus, we assessed the ability to detect ACP using a single-step approach. In the single-step reaction, we incubated the ACP simultaneously with AAP, Pt nanozymes, and TMB for 15 min. Similar to that observed for the two-step reaction, the intensity of the blue product decreased linearly as a function of increasing ACP enzyme concentration in the 0.5 to 15 mU mL^{-1} range (Fig. 2 – Blue ○). More interestingly, the single-step reaction could cut down the total reaction time by ~60%.

Although the reliance on the blue charge transfer product of TMB is common during the development of nanozyme sensors, it has two practical challenges – (i) the absorbance of the blue product changes (generally increases) with time as more product continues to be formed over time, making the assay time-sensitive; and (ii) conversely, it has also been suggested that the absorbance maximum of the blue product may not necessarily be stable over time, as it can also spontaneously revert to its colorless form.[41,62] A simple strategy to negate these challenges is to convert the blue charge transfer product to its double-oxidised, yellow diimine derivative (λ_{max} = 450 nm) by exposing the reaction to concentrated sulphuric acid. In this process, the blue charge transfer complex and other TMB intermediates are completely dissociated by the addition of an acid, simultaneously shifting the equilibrium towards the yellow product.[63] Concentrated H$_2$SO$_4$ also acts as a stop-agent, thus blocking further change in absorbance over time. This simple step can improve the stability of the analytical signal. Further, the yellow product has a higher extinction
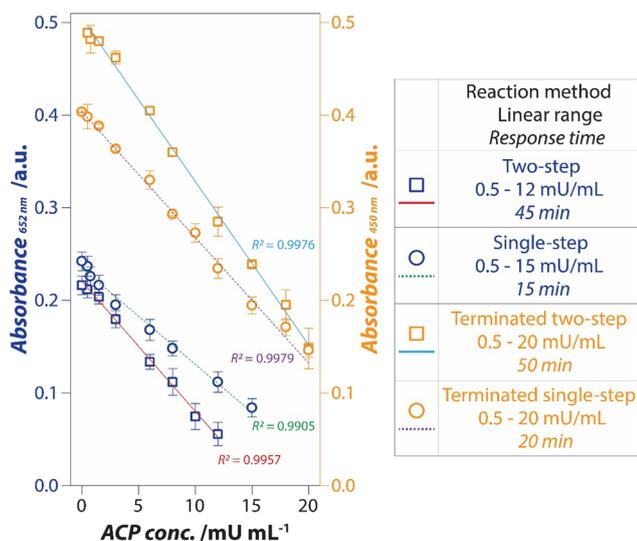

Fig. 2 Improvement in the detection of ACP was achieved by shifting from a two-step reaction to a single-step reaction (pH 5.0), further by a reaction termination approach.

coefficient (ε_{450nm} = 59 000 M^{-1} cm^{-1}) than the blue product (ε_{652nm} = 39 000 M^{-1} cm^{-1}), which should also, in principle, improve the sensitivity of the sensor. To understand if this is indeed the case, concentrated sulphuric acid was added to the reaction after the incubation time. As seen in Fig. 2, the conversion of the blue product to the yellow diimine increased the slope of the linear curves which expanded the ACP detection range to 20 mU mL^{-1} in both the single-step and two-step assays (Fig. 2 – Orange □ and ○). In both cases, the sensor response saturated beyond the ACP concentrations of 20 mU mL^{-1} (Fig. S6†). Nevertheless, this simple control over the reaction not only improved the linear dynamic range but also reduced the standard deviation during ACP detection. The latter can be attributed to the stable nature of the yellow diimine over the blue charge transfer complex. A brief comparison of the ACP detection range and time taken for the reaction using nanozyme-based assays (Table 1) shows that the current approach shows comparable sensing performance, while significantly reducing the time taken for the reaction completion.

3.6 Mechanism of ACP sensing by Pt nanozyme

Considering that ascorbic acid can either scavenge ROS or act as a reducing agent, we next determined which of these two pathways mechanistically dominate during the sensor operation. To assess the probability of these mechanisms, two independent assays were performed (Fig. 3a). In assay 1, PtNPs and TMB were allowed to react, and the reaction was monitored as a function of time. The PtNPs catalysed the oxidation of TMB *via* the generation of $^1O_2$, which increased the absorbance (Fig. 3a – Blue □). After 14 min of incubation, a fixed concentration of ascorbic acid was added to the reaction. If ascorbic acid would have acted as a reducing agent, it would convert the blue TMB back to colorless TMB resulting in a decrease in its absorbance with time (Fig. 3a – Green □). In this case, the absorbance was reduced by 24% over 14 min. In assay 2, a fixed concentration of ascorbic acid was added along with PtNPs and TMB from the beginning of the assay. In this case, the ascorbic acid would capture the $^1O_2$ species, as it is produced by PtNPs, and thus, $^1O_2$ will be inaccessible by TMB, thereby inhibiting TMB oxidation. The oxidation of TMB in the presence of ascorbic acid is significantly slower (Fig. 3a – Red ○) when compared to that in the absence of ascorbic acid (Fig. 3a – Blue □). If we compare the initial rate of the reaction with and without ascorbic acid, the rate is ~5 times lower in the presence of ascorbic acid (1.8 × 10^{-2} *vs.* 8.7 × 10^{-2} min^{-1} for the first 6 min of reaction). This suggests that the ROS scavenging activity of ascorbic acid plays a dominant role in the proposed detection of ACP.[64,65] Further, to probe the efficiency of ascorbic acid to capture $^1O_2$, an ascorbic acid concentration-dependent assay was conducted using the $^1O_2$ probe, ABDA. The production of $^1O_2$ due to the nanozyme activity of PtNPs decreased the absorbance intensity of ABDA (Fig. 3b – Red bar). When the same reaction was carried out in the presence of different concentrations of ascorbic acid, the scavenging activity of ascorbic acid resulted in less photobleaching of ABDA (Fig. 3b – Blue bars). The absorbance intensity was dependent on the concentration of ascorbic acid used in the reaction. This concentration-dependent response correlates well with our observations in the sensing experiments. Based on these observations, we can articulate that in both the single-step and the two-step approaches for the detection of ACP, the ascorbic acid produced *in situ* acts as a scavenger and inhibits the oxidation of TMB.
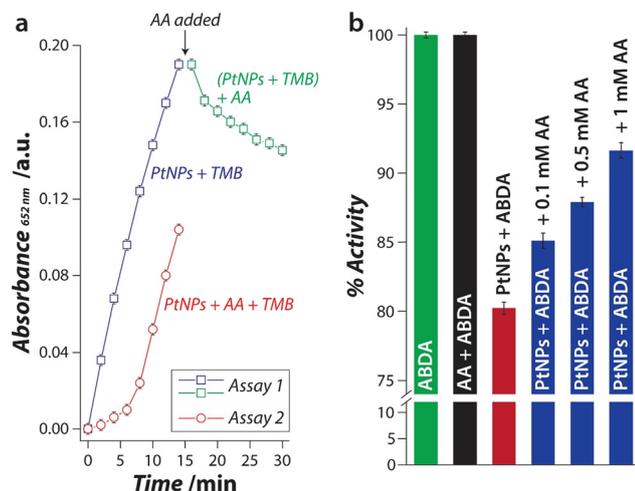
3.7 Sensor selectivity and ability to operate in a complex sample matrix

The selectivity of the sensor to specifically detect ACP was assessed by exposing the sensor to a variety of enzymes and biomolecules that may be present in biological samples. The ability of Pt nanozyme to oxidise TMB was first assessed in the presence of each interfering species such as glucose-6-phosphate dehydrogenase (G6PDH), glucose oxidase (GOX), horseradish peroxidase (HRP), pepsin, pancreatin, catalase, trypsin, glucose, and uric acid. When Pt nanozyme was exposed to these interferents, in most cases, the activity of PtNPs was not inhibited (Fig. 4a), except when the nanozyme was exposed to ACP (~30%). Similarly, when the same assay was carried out in the presence of both ACP and the interfering species, the sensor showed excellent selectivity with an interference of 5–8% (Fig. 4b). This suggests that the sensor has high selectivity to detect ACP even in the presence of interfering species.
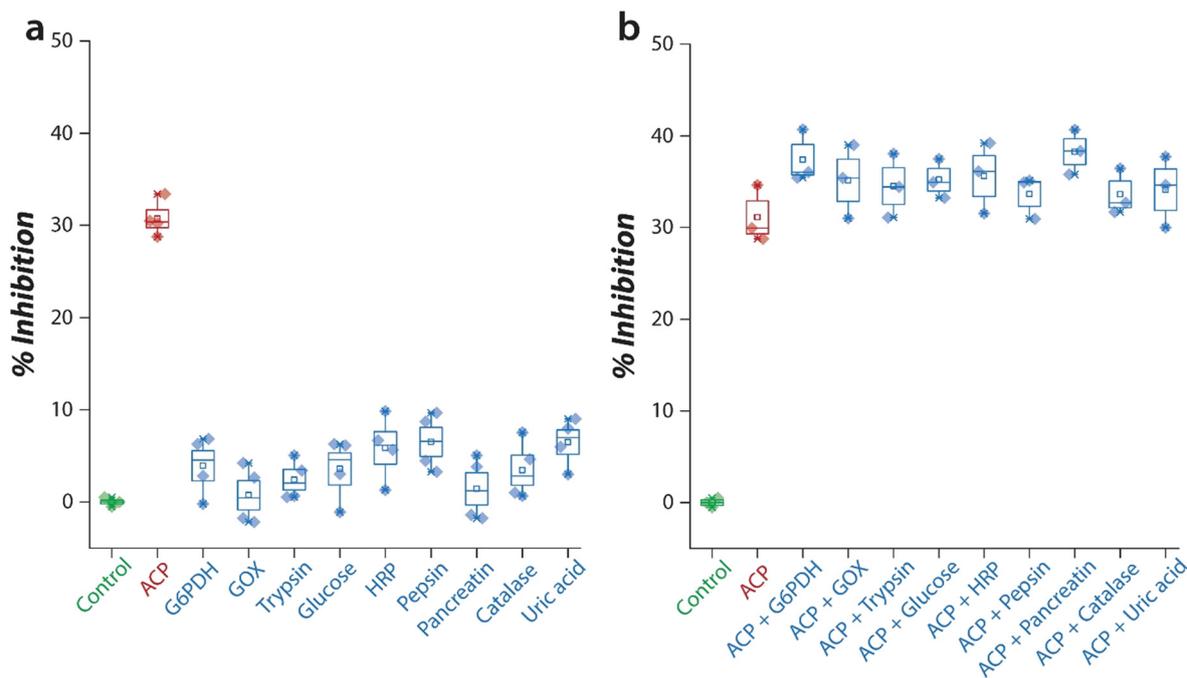

Fig. 3 Effect of ascorbic acid (AA) on the nanozyme activity of PtNPs at pH 5.0. (a) Comparison of the dual behaviour of ascorbic acid (reducing agent and radical scavenger) on the oxidase-mimic catalytic activity of PtNPs measured as a function of oxidised TMB product (λ_{max} = 652 nm). (b) AA concentration-dependent assay to test its efficiency as a $^1O_2$ scavenger.

Fig. 4 ACP sensor response when exposed to enzymes and biomolecules (a) independently and (b) in combination with ACP (reaction conditions: concentration of ACP 10 mU mL^{-1}, terminated single-step reaction, pH 5.0).

Next, the practical applicability of the Pt nanozyme sensor was assessed by detecting ACP concentrations in a relevant biological fluid, human urine. Human urine is rich in ACP as this enzyme is secreted from two organs, *viz.*, kidney and prostate.[4,6] This makes urine a good sample matrix for monitoring multiple disease conditions. Two sets of experiments were performed, initially a proof-of-concept experiment in a pH 5.0 buffer to check the viability of the proposed concept, and later an optimised experiment in a pH 4.0 buffer to obtain a practically viable detection range for ACP detection. To establish the proof of the concept, a urine sample was first collected from a healthy volunteer and centrifuged to remove any cells and other debris. The sample was then diluted 50× and spiked with a known concentration of ACP to achieve a range of 0.5 to 20 mU mL^{-1} ACP in the reaction. Table S1† summarises the estimated concentration of ACP by the Pt nanozyme. The sensor showed a recovery between 96–104% indicating the suitability of the Pt nanozyme sensor system for urine analysis of ACP. However, since ACP was added to urine post-dilution, considering the dilution factor, the corresponding ACP concentration in the urine would have been 500 to 20 000 mU mL^{-1}. This is much higher than the physiologically relevant ranges of ACP which have been reported to be 4–5 mU mL^{-1} in males aged <13 and >50 years, 11–30 mU mL^{-1} in the 13–50 age group, and 7–11 mU mL^{-1} in the case of females.[6] Therefore, we assessed the ability of the sensor to operate with minimal urine dilution. However, a desirable sensitivity could not be achieved at pH 5.0 (data not shown).

Since Pt nanozyme has a significantly higher activity at pH 4.0 (Fig. S2b†), the sensitivity of the assay without significant

urine dilution was assessed in a pH 4.0 buffer (Fig. 5). For this, known amounts (dry weight) of ACP were first added to the centrifuged urine sample to achieve urine ACP concentration of 2–100 mU mL^{-1}. These urine samples were then directly used in the proposed nanozyme assay (25 µL ACP-spiked urine +175 µL other reagents). Similar to the observations at pH 5.0 (Fig. 2), a consistent decrease in the absorbance was also observed at pH 4.0 (Fig. 5). However, at pH 4.0, the sensor response followed a concentration-
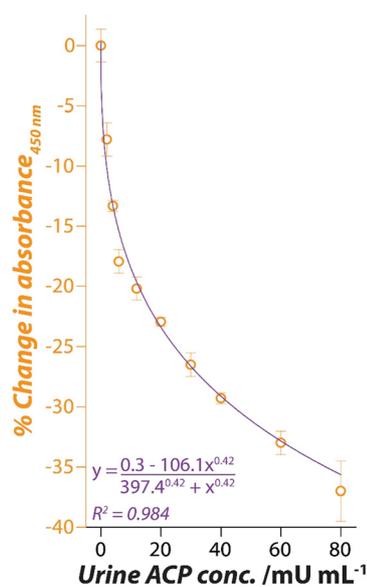

Fig. 5 Hill function fitting of the Pt nanozyme sensor response when exposed to ACP spiked urine sample at pH 4.0.

dependent non-linear trend that could be fitted with the Hill function with a high confidence. The sensor showed an operational dynamic range of 2–80 mU mL^{-1} following which the response started to saturate. This operational range is well within the biologically relevant ranges of ACP in both males and females.

Another key determinant is the interference from ascorbic acid (AA) in urine analysis, especially in the case of dipsticks or test strips.[66] The normal range of AA in urine is typically below 0.56 mM.[67] In the current case, due to the addition of the buffer containing TMB, AAP and the nanozyme, the urine samples containing ACP would have a dilution of 8× during the assay. This would mean that the concentration of AA, if present, would be <0.07 mM. Based on the data shown in Fig. 3b, such low concentrations would have a negligible effect on the sensing response. For instance, 0.1 mM AA only changes the sensor response by 5%. Hence, we could assume that the effect of AA or other antioxidants that may be present in the urine would be negligible on the sensing assay.

4. Conclusions

In summary, this study has explored the application of the oxidase-mimic catalytic activity of citrate-capped PtNPs to develop a simple colorimetric sensing platform for ACP detection. The citrate reduction method to synthesize Pt nanozymes, allows precise control over the nanoparticle size and morphology, while providing high stability in acidic medium. Platinum is one of the best-known catalysts and is already used in a series of industrial and commercial applications, such as those in catalytic converters to minimise the degree of pollution caused by vehicles. In the context of nanozyme activity, it is well established that Pt nanoparticles possess an exceptional enzyme-mimicking catalytic activity over other nanomaterials. Thus, it is of no surprise that Pt nanoparticles have been extensively reported for their multi-functional nanozyme activity, which offers Pt nanozymes a high degree of versatility in their catalytic activities.[19] This combined with their relatively non-toxic nature makes them invaluable for a wide range of chemical and biological applications. Despite one potential drawback of the high cost associated with platinum, it is worth considering that in the proposed ACP sensor, only a small amount of Pt nanoparticles is used. Therefore, the potential benefits associated with the high catalytic activity of the Pt nanozyme are expected to outweigh the cost disadvantage. The Pt nanozyme oxidises TMB to a blue product through the generation of $^1O_2$ oxygen. However, in the presence of ACP, the oxidation of TMB is inhibited due to the antioxidant ability of ascorbic acid that is produced *in situ* during the reaction. This concept allows the development of a colorimetric sensor for ACP. The optimal operating conditions of the Pt nanozyme at mildly acidic pH overlap with the activity of ACP, thus allowing the sensor to operate

in a single step. This simplified the assay workflow and reduced the assay time by half. Further, the conversion of the blue charge transfer product to a yellow diimine product by a simple treatment with sulphuric acid assisted in reducing the variability in assays. The sensor showed an excellent performance to detect 2–80 mU mL^{-1} concentration of ACP in human urine, which is well within the physiologically relevant range of 4–30 mU mL^{-1} suggesting that the newly developed Pt nanozyme sensor may be potentially used in urinalysis. This, in combination with the simplicity of conducting the test assay in a single step along with a faster sensor response of 20 min make the Pt nanozyme sensor a suitable ACP detection platform. We, however, note that early studies on urinary ACP have reported that for ACP determination, the urine sample needs to be collected in three parts, as the first and last part of micturition contains prostatic secretion that is indicative of prostatic ACP in the urine sample. It has been presumed that the mid-stream urine, which has 2–7 times lower ACP concentration than the first and the final part, is reasonably free of prostatic secretions and therefore almost entirely contains renal excretion.[4] Therefore, sampling of specific portions of the urine offers an opportunity to selectively determine the concentrations of ACP released by the prostate and kidney. This could be important as the concentrations of prostatic and renal ACP could act as biomarkers for different diseases. However, to our knowledge, the optimum strategy for urine collection to minimise, and preferably completely avoid prostatic secretions in the urine has not been developed. Large cohort studies are required to establish a baseline for urinary (prostatic and renal) ACP levels that are specific to genders, age groups, and healthy *vs.* disease conditions; the aspects that are beyond the scope of this work. Nevertheless, the development of a urinary ACP detection platform, as shown here is the first step in understanding the significance of ACP excreted in urine and thereby monitoring renal and prostatic health. Additionally, unlike serum ACP, urinary ACP monitoring offers a non-invasive approach that is conducive to more flexible sampling conditions, for instance, allowing urine collection at homes, and colorimetric monitoring can, of course, play an additional favourable role in the eventual practical deployment of such point-of-care diagnostic (POCD) systems.

Ethics declarations

Urine samples from three individuals were collected at RMIT University. The study was approved by the RMIT University's Science, Engineering and Health College Human Ethics Advisory Network (CHEAN) – project number 25839. All volunteers were provided with a detailed description of the study and a signed informed consent was collected from each volunteer before the urine samples were collected.

Data availability

Data will be made available on request.

Author contributions

Sanjana Naveen Prasad: investigation, validation, visualization, formal analysis, data curation, writing – original draft. Sanje Mahasivam: investigation, formal analysis, data curation, writing – original draft. Sabeen Hashmi: investigation, formal analysis, data curation, writing – original draft. Vipul Bansal: methodology, conceptualization, supervision, formal analysis, writing – review & editing, project administration, funding acquisition. Rajesh Ramanathan: methodology, conceptualization, supervision, formal analysis, writing – review & editing, project administration, funding acquisition.

Conflicts of interest

The authors declare that they have no known competing financial interests or personal relationships that could have appeared to influence the work reported in this paper.

Acknowledgements

References

1 H. Bull, P. G. Murray, D. Thomas, A. M. Fraser and P. N. Nelson, Acid phosphatases, *Mol. Pathol.*, 2002, **55**, 65, DOI: **10.1136/mp.55.2.65**.

2 H. Y. Kong and J. Byun, Emerging roles of human prostatic acid phosphatase, *Biomol. Ther.*, 2013, **21**, 10, DOI: **10.4062/biomolther.2012.095**.

3 L. T. Yam, Clinical significance of the human acid phosphatases: A review, *Am. J. Med.*, 1974, **56**, 604, DOI: **10.1016/0002-9343(74)90630-5**.

4 O. Daniel, P. R. Kind and E. J. King, Urinary excretion of acid phosphatase, *Br. Med. J.*, 1954, **1**, 19, DOI: **10.1136/bmj.1.4852.19**.

5 H. J. Kramer, J. E. Wight, W. L. Paul and H. C. Gonick, Studies of Human Kidney and Urine Acid Phosphatase, *Enzymol. Biol. Clin.*, 1970, **11**, 435, DOI: **10.1159/000458383**.

6 W. W. Scott and C. Huggins, The acid phosphatase activity of human urine, an index of prostatic secretion, *Endocrinology*, 1942, **30**, 107, DOI: **10.1210/endo-30-1-107**.

7 Y. Yamauchi, M. Ido and H. Maeda, High performance liquid chromatography equipped with a cathodic detector and column-switching device as a high-throughput method for a phosphatase assay with p-nitrophenyl phosphate, *J. Chromatogr. A*, 2005, **1066**, 127, DOI: **10.1016/j.chroma.2005.01.071**.

8 Z. Wajsman, T. M. Chu, J. Saroff, N. Slack and G. P. Murphy, Two new, direct, and specific methods of acid phosphatase determination National field trial, *Urology*, 1979, **13**, 8, DOI: **10.1016/0090-4295(79)90003-7**.

9 H.-H. Deng, X.-L. Lin, Y.-H. Liu, K.-L. Li, Q.-Q. Zhuang, H.-P. Peng, A.-L. Liu, X.-H. Xia and W. Chen, Chitosan-stabilized platinum nanoparticles as effective oxidase mimics for colorimetric detection of acid phosphatase, *Nanoscale*, 2017, **9**, 10292, DOI: **10.1039/C7NR03399K**.

10 X. Li, B. Li, J. Hong and X. Zhou, Highly selective determination of acid phosphatase in biological samples using a biomimetic recognition-based SERS sensor, *Sens. Actuators, B*, 2018, **276**, 421, DOI: **10.1016/j.snb.2018.08.076**.

11 S. Li, X. Hu, Q. Chen, X. Zhang, H. Chai and Y. Huang, Introducing bifunctional metal-organic frameworks to the construction of a novel ratiometric fluorescence sensor for screening acid phosphatase activity, *Biosens. Bioelectron.*, 2019, **137**, 133, DOI: **10.1016/j.bios.2019.05.010**.

12 S. R. Ahmed and A. Chen, In Situ Enzymatic Generation of Gold Nanoparticles for Nanozymatic Label-free Detection of Acid Phosphatase, *ACS Appl. Nano Mater.*, 2020, **3**, 9462, DOI: **10.1021/acsanm.0c02067**.

13 J. Wang, Q. Lu, C. Weng, X. Li, X. Yan, W. Yang, B. Li and X. Zhou, Label-Free Colorimetric Detection of Acid Phosphatase and Screening of Its Inhibitors Based on Biomimetic Oxidase Activity of MnO2 Nanosheets, *ACS Biomater. Sci. Eng.*, 2020, **6**, 3132, DOI: **10.1021/acsbiomaterials.0c00217**.

14 A. Roda, E. Michelini, M. Zangheri, M. Di Fusco, D. Calabria and P. Simoni, Smartphone-based biosensors: A critical review and perspectives, *TrAC, Trends Anal. Chem.*, 2016, **79**, 317, DOI: **10.1016/j.trac.2015.10.019**.

15 S. Naveen Prasad, S. R. Anderson, M. V. Joglekar, A. A. Hardikar, V. Bansal and R. Ramanathan, Bimetallic nanozyme mediated urine glucose monitoring through discriminant analysis of colorimetric signal, *Biosens. Bioelectron.*, 2022, **212**, 114386, DOI: **10.1016/j.bios.2022.114386**.

16 M. Sánchez, A. González, L. Sabio, W. Zou, R. Ramanathan, V. Bansal and J. M. Dominguez-Vera, Photochromic polyoxometalate–based enzyme-free reusable sensors for real-time colorimetric detection of alcohol in sweat and saliva, *Mater. Today Chem.*, 2021, **21**, 100491, DOI: **10.1016/j.mtchem.2021.100491**.

17 E. Engvall and P. Perlmann, Enzyme-linked immunosorbent assay (ELISA) quantitative assay of immunoglobulin G, *Immunochemistry*, 1971, **8**, 871, DOI: **10.1016/0019-2791(71)90454-X**.

18 H. Wei and E. Wang, Nanomaterials with enzyme-like characteristics (nanozymes): next-generation artificial enzymes, *Chem. Soc. Rev.*, 2013, **42**, 6060, DOI: **10.1039/C3CS35486E**.

19 J. Wu, X. Wang, Q. Wang, Z. Lou, S. Li, Y. Zhu, L. Qin and H. Wei, Nanomaterials with enzyme-like characteristics (nanozymes): next-generation artificial enzymes (II), *Chem. Soc. Rev.*, 2019, **48**, 1004, DOI: **10.1039/C8CS00457A**.

20 Y. Lin, J. Ren and X. Qu, Catalytically active nanomaterials: A promising candidate for artificial enzymes, *Acc. Chem. Res.*, 2014, **47**, 1097, DOI: **10.1021/ar400250z**.

21 M. Nasir, M. H. Nawaz, U. Latif, M. Yaqub, A. Hayat and A. Rahim, An overview on enzyme-mimicking nanomaterials for use in electrochemical and optical assays, *Microchim. Acta*, 2017, **184**, 323, DOI: **10.1007/s00604-016-2036-8**.

22 M. N. Karim, S. R. Anderson, S. Singh, R. Ramanathan and V. Bansal, Nanostructured silver fabric as a free-standing NanoZyme for colorimetric detection of glucose in urine, *Biosens. Bioelectron.*, 2018, **110**, 8, DOI: **10.1016/j.bios.2018.03.025**.

23 M. N. Karim, M. Singh, P. Weerathunge, P. Bian, R. Zheng, C. Dekiwadia, T. Ahmed, S. Walia, E. Della Gaspera, S. Singh, R. Ramanathan and V. Bansal, Visible-Light-Triggered Reactive-Oxygen-Species-Mediated Antibacterial Activity of Peroxidase-Mimic CuO Nanorods, *ACS Appl. Nano Mater.*, 2018, **1**, 1694, DOI: **10.1021/acsanm.8b00153**.

24 S. Naveen Prasad, P. Weerathunge, M. N. Karim, S. Anderson, S. Hashmi, P. D. Mariathomas, V. Bansal and R. Ramanathan, Non-invasive detection of glucose in human urine using a color-generating copper NanoZyme, *Anal. Bioanal. Chem.*, 2021, **413**, 1279, DOI: **10.1007/s00216-020-03090-w.**

25 P. D. Liyanage, P. Weerathunge, M. Singh, V. Bansal and R. Ramanathan, L-Cysteine as an Irreversible Inhibitor of the Peroxidase-Mimic Catalytic Activity of 2-Dimensional Ni-Based Nanozymes, *Nanomaterials*, 2021, **11**, 1285, DOI: **10.3390/nano11051285.**

26 M. Singh, P. Weerathunge, P. D. Liyanage, E. Mayes, R. Ramanathan and V. Bansal, Competitive inhibition of the enzyme-mimic activity of Gd-based nanorods toward highly specific colorimetric sensing of l-cysteine, *Langmuir*, 2017, **33**, 10006, DOI: **10.1021/acs.langmuir.7b01926.**

27 P. Weerathunge, B. K. Behera, S. Zihara, M. Singh, S. Naveen Prasad, S. Hashmi, P. R. D. Mariathomas, V. Bansal and R. Ramanathan, Dynamic interactions between peroxidase-mimic silver NanoZymes and chlorpyrifos-specific aptamers enable highly-specific pesticide sensing in river water, *Anal. Chim. Acta*, 2019, **1083**, 157, DOI: **10.1016/j.aca.2019.07.066.**

28 P. Weerathunge, R. Ramanathan, R. Shukla, T. K. Sharma and V. Bansal, Aptamer-controlled reversible inhibition of gold nanozyme activity for pesticide sensing, *Anal. Chem.*, 2014, **86**, 11937, DOI: **10.1021/ac5028726.**

29 P. Weerathunge, R. Ramanathan, V. A. Torok, K. Hodgson, Y. Xu, R. Goodacre, B. K. Behera and V. Bansal, Ultrasensitive colorimetric detection of murine norovirus using NanoZyme

aptasensor, *Anal. Chem.*, 2019, **91**, 3270, DOI: **10.1021/acs.analchem.8b03300**.

30 P. Weerathunge, T. K. Sharma, R. Ramanathan and V. Bansal, *Nanozyme-Based Environmental Monitoring*, The Royal Society of Chemistry, 2016, p. 108, DOI: **10.1039/9781782629139-00108**.

31 T. K. Sharma, R. Ramanathan, P. Weerathunge, M. Mohammadtaheri, H. K. Daima, R. Shukla and V. Bansal, Aptamer-mediated "turn-off/turn-on" nanozyme activity of gold nanoparticles for kanamycin detection, *Chem. Commun.*, 2014, **50**, 15856, DOI: **10.1039/c4cc07275h**.

32 S. Naveen Prasad, V. Bansal and R. Ramanathan, Detection of pesticides using nanozymes: trends, challenges and outlook, *TrAC, Trends Anal. Chem.*, 2021, 116429, DOI: **10.1016/j.trac.2021.116429**.

33 S. Naveen Prasad, V. Bansal and R. Ramanathan, in *Nanozyme-Based Sensors for Pesticide Detection*, ed. H. K. Daima, N. Pn and E. Lichtfouse, Springer International Publishing, Cham, 2021, p. 145, DOI: **10.1007/978-3-030-68230-9_6**.

34 S. Hashmi, M. Singh, P. Weerathunge, E. L. H. Mayes, P. D. Mariathomas, S. Naveen Prasad, R. Ramanathan and V. Bansal, Cobalt Sulfide Nanosheets as Peroxidase Mimics for Colorimetric Detection of l-Cysteine, *ACS Appl. Nano Mater.*, 2021, **4**, 13352, DOI: **10.1021/acsanm.1c02851**.

35 X. Tao, X. Wang, B. Liu and J. Liu, Conjugation of antibodies and aptamers on nanozymes for developing biosensors, *Biosens. Bioelectron.*, 2020, **168**, 112537, DOI: **10.1016/j.bios.2020.112537**.

36 K. Fan, Y. Lin and V. Bansal, Editorial: Nanozymes: From Rational Design to Biomedical Applications, *Front. Chem.*, 2021, **9**, 670767, DOI: **10.3389/fchem.2021.670767**.

37 B. Liu and J. Liu, Surface modification of nanozymes, *Nano Res.*, 2017, **10**, 1125, DOI: **10.1007/s12274-017-1426-5**.

38 Q. Wang, H. Wei, Z. Zhang, E. Wang and S. Dong, Nanozyme: An emerging alternative to natural enzyme for biosensing and immunoassay, *TrAC, Trends Anal. Chem.*, 2018, **105**, 218, DOI: **10.1016/j.trac.2018.05.012**.

39 H. Wei, L. Gao, K. Fan, J. Liu, J. He, X. Qu, S. Dong, E. Wang and X. Yan, Nanozymes: A clear definition with fuzzy edges, *Nano Today*, 2021, **40**, 101269, DOI: **10.1016/j.nantod.2021.101269**.

40 R. Walther, A. K. Winther, A. S. Fruergaard, W. van den Akker, L. Sørensen, S. M. Nielsen, M. T. J. Olesen, Y. Dai, H. S. Jeppesen, P. Lamagni, A. Savateev, S. L. Pedersen, C. K. Frich, C. Vigier-Carrière, N. Lock, M. Singh, V. Bansal, R. L. Meyer and A. N. Zelikin, Identification and Directed Development of Non-Organic Catalysts with Apparent Pan-Enzymatic Mimicry into Nanozymes for Efficient Prodrug Conversion, *Angew. Chem., Int. Ed.*, 2019, **58**, 278, DOI: **10.1002/anie.201812668**.

41 M. Drozd, M. Pietrzak, P. G. Parzuchowski and E. Malinowska, Pitfalls and capabilities of various hydrogen donors in evaluation of peroxidase-like activity of gold nanoparticles, *Anal. Bioanal. Chem.*, 2016, **408**, 8505, DOI: **10.1007/s00216-016-9976-z**.

42 Y. Chong, Q. Liu and C. Ge, Advances in oxidase-mimicking nanozymes: Classification, activity regulation and biomedical applications, *Nano Today*, 2021, **37**, 101076, DOI: **10.1016/j.nantod.2021.101076**.

43 B. Valderrama, M. Ayala and R. Vazquez-Duhalt, Suicide inactivation of peroxidases and the challenge of engineering more robust enzymes, *Chem. Biol.*, 2002, **9**, 555, DOI: **10.1016/S1074-5521(02)00149-7**.

44 L. Jin, Y. Sun, L. Shi, C. Li and Y. Shen, PdPt bimetallic nanowires with efficient oxidase mimic activity for the colorimetric detection of acid phosphatase in acidic media, *J. Mater. Chem. B*, 2019, **7**, 4561, DOI: **10.1039/C9TB00730J**.

45 W. Patungwasa and J. H. Hodak, pH tunable morphology of the gold nanoparticles produced by citrate reduction, *Mater. Chem. Phys.*, 2008, **108**, 45, DOI: **10.1016/j.matchemphys.2007.09.001**.

46 A. M. Alkilany, S. R. Abulateefeh, K. K. Mills, A. I. Bani Yaseen, M. A. Hamaly, H. S. Alkhatib, K. M. Aiedeh and J. W. Stone, Colloidal Stability of Citrate and Mercaptoacetic Acid Capped Gold Nanoparticles upon Lyophilization: Effect of Capping Ligand Attachment and Type of Cryoprotectants, *Langmuir*, 2014, **30**, 13799, DOI: **10.1021/la504000v**.

47 X. Liu, H. Ding, B. Hu, F. Tian, J. Sun, L. Jin and R. Yang, Large-scale synthesis of high loading Co single-atom catalyst with efficient oxidase-like activity for the colorimetric detection of acid phosphatase, *Appl. Surf. Sci.*, 2022, **605**, 154766, DOI: **10.1016/j.apsusc.2022.154766**.

48 Z. Lin, X. Zhang, S. Liu, L. Zheng, Y. Bu, H. Deng, R. Chen, H. Peng, X. Lin and W. Chen, Colorimetric acid phosphatase sensor based on MoO3 nanozyme, *Anal. Chim. Acta*, 2020, **1105**, 162, DOI: **10.1016/j.aca.2020.01.035**.

49 Y. Zhang, S. Yang, J. Wang, Y. Cai, L. Niu, X. Liu, C. Liu, H. Qi and A. Liu, Copper sulfide nanoclusters with multi-enzyme-like activities and its application in acid phosphatase sensing based on enzymatic cascade reaction, *Talanta*, 2021, **233**, 122594, DOI: **10.1016/j.talanta.2021.122594**.

50 S. Zheng, H. Gu, D. Yin, J. Zhang, W. Li and Y. Fu, Biogenic synthesis of AuPd nanocluster as a peroxidase mimic and its application for colorimetric assay of acid phosphatase, *Colloids Surf., A*, 2020, **589**, 124444, DOI: **10.1016/j.colsurfa.2020.124444**.

51 Y. Guo, X. Li, Y. Dong and G.-L. Wang, Acid Phosphatase Invoked Exquisite Enzyme Cascade for Amplified Colorimetric Bioassay, *ACS Sustainable Chem. Eng.*, 2019, **7**, 7572, DOI: **10.1021/acssuschemeng.8b05719**.

52 X. Liu, L. Yan, H. Ren, Y. Cai, C. Liu, L. Zeng, J. Guo and A. Liu, Facile synthesis of magnetic hierarchical flower-like Co3O4 spheres: Mechanism, excellent tetra-enzyme mimics and their colorimetric biosensing applications, *Biosens. Bioelectron.*, 2020, **165**, 112342, DOI: **10.1016/j.bios.2020.112342**.

53 D. Yang, J. Chen, Y. Huang, G. Chen, X. Liu, X. Wang, L. Yang, Z. Li, J. Hu, Q. Zhou, J. Ge and Y. Yang, Oxidase-like Fe–N/C single atom nanozyme enables sensitive detection of ascorbic acid and acid phosphatase, *Anal. Chim. Acta*, 2023, **1265**, 341221, DOI: **10.1016/j.aca.2023.341221**.

54 X. Zhao, Z. Li, S. N. Wang, Z. Yuan and Y. Lu, Bimetallic synergistic Pd-Pt icosahedra as highly active peroxidase-like mimics for colorimetric analysis, *ChemPhysMater*, 2023, **2**, 295, DOI: **10.1016/j.chphma.2023.05.002**.

55 C. Chen, W. Liu, P. Ni, Y. Jiang, C. Zhang, B. Wang, J. Li, B. Cao, Y. Lu and W. Chen, Engineering Two-Dimensional Pd Nanoplates with Exposed Highly Active {100} Facets Toward Colorimetric Acid Phosphatase Detection, *ACS Appl. Mater. Interfaces*, 2019, **11**, 47564, DOI: **10.1021/acsami.9b16279**.

56 S.-B. He, L. Yang, Y. Yang, H. A. A. Noreldeen, G.-W. Wu, H.-P. Peng, H.-H. Deng and W. Chen, Carboxylated chitosan enabled platinum nanozyme with improved stability and ascorbate oxidase-like activity for a fluorometric acid phosphatase sensor, *Carbohydr. Polym.*, 2022, **298**, 120120, DOI: **10.1016/j.carbpol.2022.120120**.

57 X. Qiao, H. Li, H. Ma, H. Zhang and L. Jin, Sensitive acid phosphatase assay based on light-activated specific oxidase mimic activity, *Talanta*, 2023, **255**, 124236, DOI: **10.1016/j.talanta.2022.124236**.

58 N. C. Bigall, T. Härtling, M. Klose, P. Simon, L. M. Eng and A. Eychmüller, Monodisperse Platinum Nanospheres with Adjustable Diameters from 10 to 100 nm: Synthesis and Distinct Optical Properties, *Nano Lett.*, 2008, **8**, 4588, DOI: **10.1021/nl802901t**.

59 Y. Zhou, B. Liu, R. Yang and J. Liu, Filling in the Gaps between Nanozymes and Enzymes: Challenges and Opportunities, *Bioconjugate Chem.*, 2017, **28**, 2903, DOI: **10.1021/acs.bioconjchem.7b00673**.

60 J. Zielonka, J. Vasquez-Vivar and B. Kalyanaraman, Detection of 2-hydroxyethidium in cellular systems: a unique marker product of superoxide and hydroethidine, *Nat. Protoc.*, 2008, **3**, 8, DOI: **10.1038/nprot.2007.473**.

61 T. Entradas, S. Waldron and M. Volk, The detection sensitivity of commonly used singlet oxygen probes in aqueous environments, *J. Photochem. Photobiol., B*, 2020, **204**, 111787, DOI: **10.1016/j.jphotobiol.2020.111787**.

62 P. D. Josephy, T. Eling and R. P. Mason, The horseradish peroxidase-catalyzed oxidation of 3, 5, 3′, 5′-tetramethylbenzidine. Free radical and charge-transfer complex intermediates, *J. Biol. Chem.*, 1982, **257**, 3669, DOI: **10.1016/S0021-9258(18)34832-4**.

63 R. A. Bally and T. Gribnau, Some aspects of the chromogen 3, 3, 5, 5-tetramethylbenzidine as hydrogen donor in a horseradish peroxidase assay, *Clin. Chem. Lab. Med.*, 1989, **27**, 791, DOI: **10.1515/cclm.1989.27.10.791**.

64 R. S. Bodannes and P. C. Chan, Ascorbic acid as a scavenger of singlet oxygen, *FEBS Lett.*, 1979, **105**, 195, DOI: **10.1016/0014-5793(79)80609-2**.

65 M. Shi, B. Xu, K. Azakami, T. Morikawa, K. Watanabe, K. Morimoto, M. Komatsu, K. Aoyama and T. Takeuchi, Dual role of vitamin C in an oxygen-sensitive system: Discrepancy between DNA damage and dell death, *Free Radical Res.*, 2005, **39**, 213, DOI: **10.1080/10715760400022129**.

66 W. Lee, Y. Kim, S. Chang, A. J. Lee and C. H. Jeon, The influence of vitamin C on the urine dipstick tests in the clinical specimens: a multicenter study, *J. Clin. Lab. Anal.*, 2017, **31**, e22080, DOI: **10.1002/jcla.22080**.

67 D.-H. Ko, T.-D. Jeong, S. Kim, H.-J. Chung, W. Lee, S. Chun and W.-K. Min, Influence of Vitamin C on Urine Dipstick Test Results, *Ann. Clin. Lab. Sci.*, 2015, **45**, 391.